Soft Matter

View Online
Dynamic Article Links

Cite this: *Soft Matter*, 2011, **7**, 2832

www.rsc.org/softmatter

PAPER

Attractive glass formation in aqueous mixtures of colloidal gibbsite platelets and silica spheres

Dzina Kleshchanok,*[a] Janne-Mieke Meijer,[a] Andrei V. Petukhov,[a] Giuseppe Portale[b] and Henk N. W. Lekkerkerker[a]

Received 26th October 2010, Accepted 15th December 2010
DOI: 10.1039/c0sm01206h

We present an experimental study on the attractive glass formation in mixtures of colloidal gibbsite platelets and silica spheres. The platelets are 233 nm in diameter, and the diameter ratio between the platelets and the spheres is 13.8. The glass formation is induced by the short-ranged depletion attraction caused by the spheres. At sufficiently high sphere concentrations the depletion attraction is strong enough that the mixtures do not form the equilibrium liquid-crystalline phases, but the glass formation occurs instead. Using microradian X-ray diffraction measurements we provide detailed information about the structure of the arrested glass state. In mixtures with weaker depletion it consists of liquid-crystalline pockets embedded in the less ordered glassy surrounding. With a stronger attraction in the system the size of these domains decreases, until the structure of the attractive glass becomes completely disordered and isotropic.

I. Introduction

Rheological properties of kinetically arrested states of anisotropic colloids, such as gels and glasses, are of large interest for the food industry,[1] pharmacy and agriculture,[2] and construction and mining industries.[3,4] For example, suspensions of natural clays find a large application in drilling fluid formulations because of their high low-shear viscosities, high yield stress and shear thinning.[3] This useful rheological response is based on the microscopic structural properties of the systems, originating from a highly anisotropic shape of colloids (rod- or platelet-like) and the interparticle interactions. Anisotropic colloids, generally, show richer phase behaviour than that of spherical colloids due to the additional orientational degree of freedom. Thus, rod- and platelet-like particles are able to form liquid-crystalline phases of various symmetries upon increasing their concentration in suspensions.[5] Further, anisotropic colloids, due to their large excluded volume, form arrested states at significantly lower volume fractions than spherical colloids.[6,7] Especially suspensions of clay particles are reported to become kinetically arrested at concentrations as low as 2 wt%.[7] In order to control and manipulate the mechanical properties of the kinetically arrested suspensions, information about their structure, as well as understanding the routes leading to their formation is essential.

There are several ways to induce the kinetical arrest in a colloidal system. Gels, for example, are formed due to attractive interactions and bonding at low particle density.[8] Glasses, on the other hand, form at high colloid concentration. In repulsive glasses diffusion of the hard core repelling colloids is disturbed by the presence of neighbouring particles, *i.e.* the particles are caged by their neighbors.[9–12] Attractive glasses form in systems with strong attraction, which is short-ranged compared to the hard core colloidal repulsion. This leads to a strong and long lasting localization of the colloids within this range and results in a kinetically arrested attractive glass.[9,10,12] Whilst the repulsive glass state has been recognized and studied for a long time,[11,13,14] the attractive glass is much more recent addition to the scientific spectrum. Attractive glasses have been experimentally studied in polymer/sphere mixtures,[15–17] in sphere suspensions with solvent mixtures near the critical point,[18] in copolymer micellar systems,[19] and in star polymer mixtures.[20] A common route is to use depletion interaction to induce attraction in colloidal systems and to facilitate the attractive glass formation. Depletion takes place when colloidal particles are mixed with another component, different in size or shape.[21] At sufficiently high concentrations of the colloid and the depletant, phase separation or kinetical arrest occurs due to the gain in free volume available to the depletant. The depth of the depletion attraction potential depends on the depletant concentration, while its range on the depletant size. Thus, the shape of the depletion potential can be effectively tuned by choosing different sizes and concentrations of the depletants. Additionally, the shape of colloidal particles influences the strength of the attraction as well. For example, a significantly stronger depletion attraction can be induced in suspensions of anisotropic colloids, such as platelets, than in suspensions of spheres, while the same amount of the depletant is used. It happens due to the fact, that

[a]*Van 't Hoff Laboratory, Debye Institute for Nanomaterials Science, Utrecht University, The Netherlands. E-mail: D.Kleshchanok@uu.nl*
[b]*Dutch Organization for Scientific Research (NWO), DUBBLE-CRG, European Synchrotron Radiation Facility (ESRF), France*

platelets touching face-to-face provide a significantly larger free volume available to the depletants than spheres. This is why one can expect that the attractive glass is formed in platelet suspensions with strong depletion attraction at sufficiently lower concentrations of both the colloidal platelets and depletants.

Here we present an experimental study on mixtures of colloidal platelets and spheres. The colloidal platelets used are inorganic gibbsite (γ-$Al(OH)_3$) particles with pronounced hexagonal shape and the diameter, D, significantly larger than the thickness, L. The experimental platelet system is simple and well characterized.[22–24] Its phase behaviour with both nematic and columnar liquid-crystalline phases has been extensively studied.[25] Furthermore, charged gibbsite platelets might be used as a model system for platelet-like clay particles which are difficult to control and to describe theoretically due to their large polydispersity in both size and shape.[26] To induce attraction in the platelet system silica spheres are used as a depletant, which are easy to manipulate experimentally. Previously, aqueous mixtures of gibbsite platelets with the small diameter and silica spheres ($D_{gibbsite}/D_{silica} = 5.7$) have been studied and the equilibrium phase diagram was established.[27] This showed that depletion attraction significantly expanded the isotropic-columnar coexistence region. Here we show under which conditions the platelet/sphere system is unable to access the liquid-crystalline phases and an arrested state is formed instead.

This is, to our knowledge, the first experimental study on the attractive glass formed by colloidal platelets. After a brief description of samples and instrumentation, we will present an experimental phase diagram of aqueous mixtures of spheres and platelets. Further, on the basis of the microradian X-ray diffraction measurements we will deduce and discuss in detail the structure of the attractive glass formed in the mixtures. To conclude, we will discuss the role of the strength and the range of the depletion attraction on the glass formation in platelet suspensions.

II. Materials and methods

Experimental system

Colloidal gibbsite platelets with a relative large diameter were synthesized in two steps. First small platelets were obtained as described by Wierenga *et al.*[22] and were grown larger in a second seeded growth step.[28] Al_{13} ions (as produced by hydrolysis of aluminium chlorohydrate, $Al_2(OH)_5Cl_2 \cdot 3H_2O$, Locron P, Hoechst AG) were adsorbed onto the gibbsite surfaces to provide them additional charge.[22] Through a sequence of three centrifugations (7 h, 1300 G) and redispersions, the excess of Al_{13} ions was removed and the platelets were brought into a 10^{-4} M NaCl solution. The gibbsite platelets are stable in aqueous solutions due to the electrostatic repulsion between them.

To induce depletion attraction between the platelets small silica spheres were added. Silica Ludox CL spheres were obtained from Sigma-Aldrich Co. The surface of Ludox CL is coated by the manufacturer with aluminium oxide, which converts the charge of the particles from negative to positive. As a result the surfaces of gibbsite platelets and silica spheres have the same charge.

The average particle diameter, $\langle D \rangle$, and the standard deviation, σ, were determined from transmission electron microscopy (TEM) images (Fig. 1a and b). Atomic force microscopy was used to obtain the thickness of the gibbsite platelets, $\langle L \rangle$. The particle characteristics are listed in Table 1.

Sample preparation

Samples were prepared by mixing the stock suspensions of gibbsite and silica with solvent such that the desired colloid concentrations were obtained. Two series of mixed gibbsite/silica suspensions were made with a constant volume percent of gibbsite (4 and 8 vol%), and a varying amount of silica, from 2.2 to 8.0 vol%. As a reference a series of pure gibbsite suspensions were prepared with a platelet concentration of 3.7 to 16.2 vol%. All suspensions were prepared with 10^{-4} M NaCl solution. For visual observations mixtures were put into flat glass capillaries (1.0 × 10.0 mm cross-section, Vitrotubes, VitroCom Inc.) that were flame sealed. Suspensions for microradian X-ray diffraction (μradXRD) experiments were placed into round Mark tubes (2 mm diameter, 10 μm wall thickness, W. Müller, Berlin). All samples were stored vertically at 20 °C. The samples liquid crystallinity was checked either with crossed polarisers or μradXRD. The phase behaviour of the systems was studied on a time scale, where sedimentation did not play a dominant role.

Microradian X-ray diffraction

X-Ray scattering experiments were performed at the European Synchrotron Radiation Facility (ESRF) in Grenoble, France, at the Dutch–Belgian beam line BM-26.[29] A microradian X-ray diffraction (μradXRD) setup was used and it is described in detail elsewhere.[30] The X-ray beam was focused by a set of beryllium compound refractive lenses (CRLs)[31] at the phosphor screen of the CCD (charge coupled device) X-ray detectors (Photonic Science, 4008 × 2671 pixels of 22 μm^2). This setup allowed an angular resolution of the order of 5–7 microradians. The beam diameter in the sample was about 0.5 mm. The capillaries were placed just after the CRLs at a distance of about 8 m from the detector. The X-ray photon energy of 13 keV (the wavelength, $\lambda = 0.0954$ nm) was used. This combination provided a range of scattering vector, q, values of $0.011\ nm^{-1} \leq q \leq 0.370\ nm^{-1}$. The modulus of the scattering vector is determined by the scattering angle 2θ as $q = 4\pi \sin\theta/\lambda$.

III. Phases and arrested states

The pure gibbsite suspensions were found to be isotropic (I) up to about 11 vol% of platelets, as these samples showed no birefringence when observed between crossed polarisers (Fig. 2a). Upon increasing the amount of platelets, we observed an isotropic/nematic (I/N) phase coexistence, then a nematic (N) phase followed by a nematic/columnar (N/C) phase coexistence. The nematic phase was recognized by being birefringent between crossed polarisers (Fig. 2b and c), while the columnar phase additionally showed Bragg reflections with white light illumination (inset in Fig. 2c). The observed phase behaviour of pure gibbsite suspensions complies well with the previous experimentally studied gibbsite systems[24,25] and is in accordance with simulations results.[32]

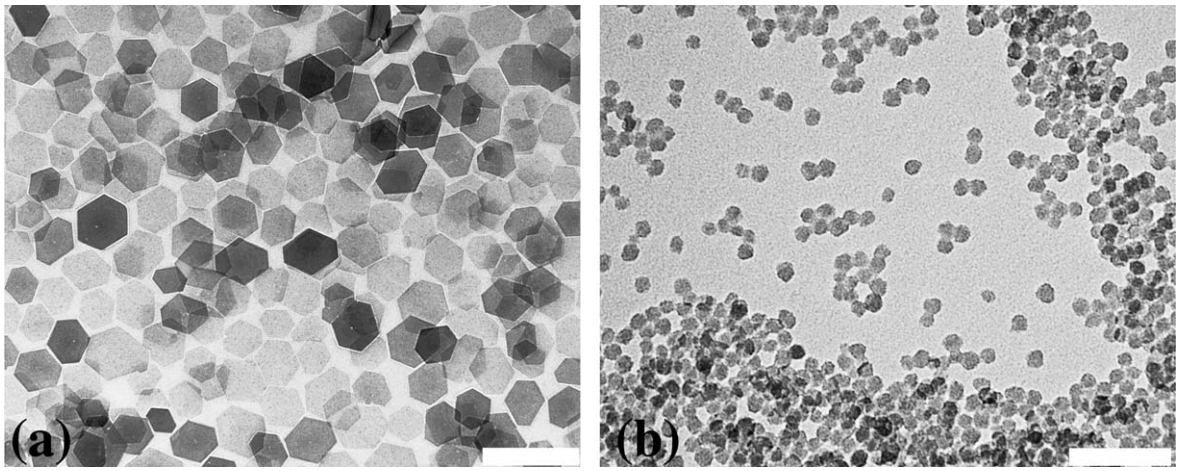

Fig. 1 Transmission electron micrographs of (a) hexagonal gibbsite platelets and (b) silica Ludox CL spheres used in this study. The scale bars are 500 nm and 100 nm respectively.

Adding above 2 vol% of silica spheres to the isotropic gibbsite suspensions caused a phase separation, which occurred in all samples already within one hour. In samples with 6.7 and higher volume percent of silica the phase separation even occurred within minutes. Micrographs of the phase separated samples are shown in Fig. 3. The amount of bottom phase increases linearly with the concentration of spheres, as is also depicted in Fig. 4 for the series of suspensions with 4 (black squares) and 8 vol% (open squares) of gibbsite. The top phase of all samples did not show birefringence between crossed polarisers, which indicates the presence of an isotropic structure. It is important to notice that the isotropic phase in suspensions with above 6.7 vol% of silica appeared totally transparent after the phase separation (Fig. 3d, e, i and j), indicating a complete absence of gibbsite platelets there.

The bottom phase of the mixtures showed no birefringence as well. However, due to high turbidity of the suspensions, the presence of a possible weak birefringence was difficult to detect. This is why the μradXRD measurements were needed to find its exact structure (see Section IV). Further, the bottom phase was very rigid and did not flow when the capillaries were tilted or were even turned upside down. This simple test tube inversion experiment already gave an indication that the bottom phase of mixed gibbsite/silica suspensions has characteristics of a kinetically arrested colloidal glass (G). The next section will give detailed insights into its structure.

To summarize, the visual observations on the pure gibbsite and mixed silica/gibbsite samples are presented in an experimental phase diagram (Fig. 5). All pure gibbsite suspensions reached their equilibrium phase behaviour. Upon increasing the platelet concentration they showed an I phase (empty squares), an I/N phase coexistence, an N phase (empty star) and an N/C phase coexistence (empty diamonds). Spheres, added to the gibbsite suspensions, act as depletants and can induce a phase separation in former isotropic samples, at sufficient sphere concentrations. Previously it was already shown that colloidal spheres significantly change the phase behaviour of platelets, by inducing a very broad I/C coexistence region.[27] However, in this case the bottom phase in mixed samples was unable to form the equilibrium liquid-crystalline phase but instead became arrested (black squares). The nature of this arrested state is an attractive glass (G), which structure will be discussed in detail in the next section. Already the pure kinetical aspects of the bottom phase formation gave a hint why it became a glass. With increasing silica concentration the time needed for a sample to form a bottom phase decreased and it took only minutes for the samples with the highest sphere concentrations. Thus, the mixed samples simply did not have enough time to form an equilibrium liquid-crystalline phase, which is usually formed within one day.[27]

Table 1 Characteristic sizes of gibbsite platelets and silica Ludox CL spheres

	$\langle D\rangle$/nm	σ_D/nm	$\langle L\rangle$/nm	σ_L/nm	
Gibbsite	232.5	34.0	8.4	2.8	$L/D = 0.04$
Silica	16.8	1.7	—	—	$D_{\text{gibbsite}}/D_{\text{silica}} = 13.8$

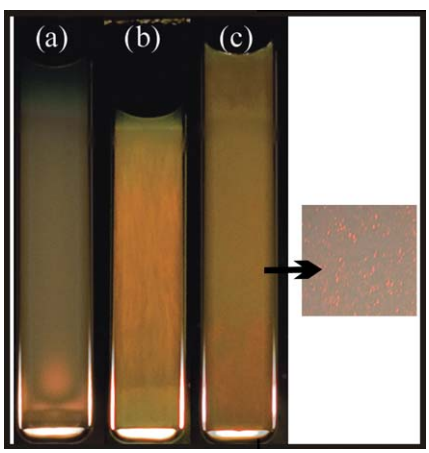

Fig. 2 Aqueous suspensions of pure gibbsite platelets observed between crossed polarisers, showing (a) an isotropic phase for 3.7 vol%, (b) a nematic phase for 12.3 vol%, and (c) a nematic/columnar phase coexistence for 16.2 vol% of platelets. The inset shows an enlarged view of the columnar phase with white light illumination.

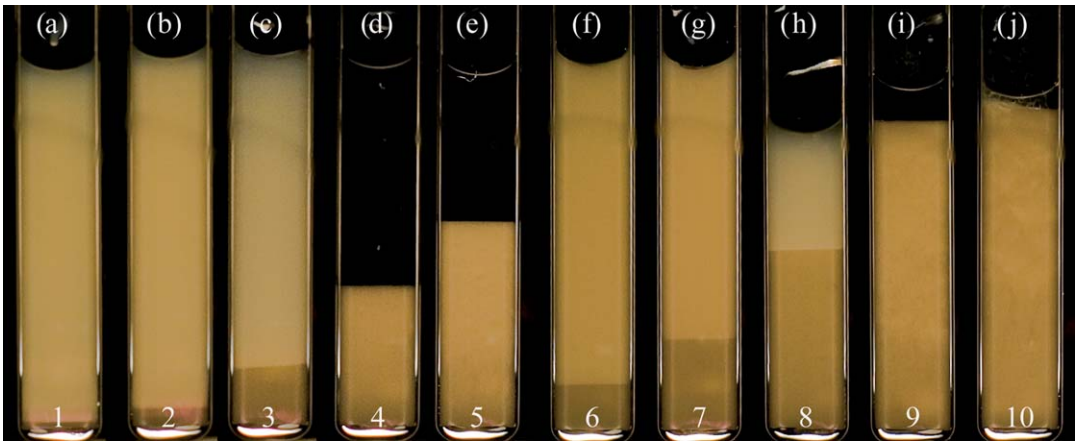

Fig. 3 Aqueous gibbsite/silica suspensions observed between crossed polarisers one day after the sample preparation. With, from (a) to (e), 4 vol% gibbsite and 2.2; 3.4; 4.9; 7.1; and 8.0 vol% silica spheres; from (f) to (j), 8 vol% of gibbsite and 2.6; 3.4; 4.4; 6.7; and 7.6 vol% silica spheres. Numbers at the bottom label the sample positions in the experimental phase diagram (Fig. 5).

The tie lines in the phase diagram, connecting coexisting isotropic and possible liquid-crystalline phases, were difficult to determine, since it was not possible to obtain samples at their equilibrium point. However, from the previous publication[27] it is known that the isotropic phase is rich in spheres, while the bottom phase is rich in platelets. Thus, the tie lines would run from the upper left to the lower right corner, being stopped at the glass transition line (dashed line in Fig. 5).

IV. Structure of the attractive glass in mixed platelet/sphere suspensions

To distinguish the exact structure of the bottom phase in silica/gibbsite suspensions we performed high resolution μradXRD measurements of the samples 6–10 (as labelled in Fig. 5). Here we will not discuss the scattering data from the isotropic phase of mixed gibbsite/silica suspensions, since their general features resemble previously published data.[27]

As mentioned in the previous section the bottom phase in suspensions 6–8 had formed within one hour, while for the two highest sphere concentrations, samples 9 and 10, the process took only a couple of minutes. Thus, the sphere concentration in the mixtures strongly affects the kinetics of the bottom phase formation and it is expected that the structure will be influenced as well. First a detailed analysis of the glass phase scattering data

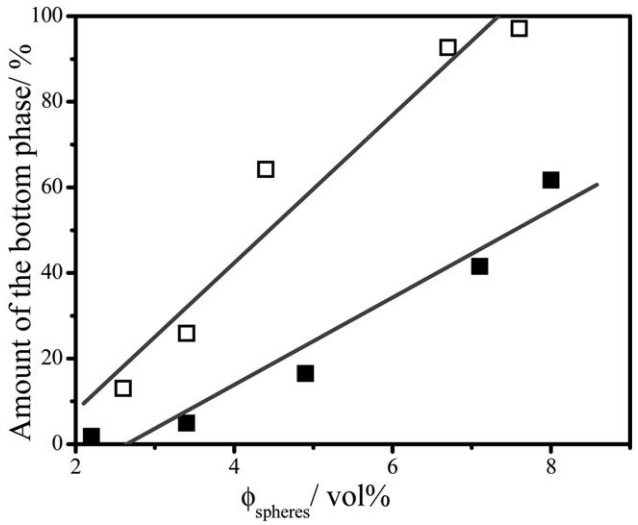

Fig. 4 Amount of the bottom phase in the platelet/sphere mixtures as function of vol% of spheres for the series of suspensions with 4 vol% (black squares) and 8 vol% (open squares) of gibbsite one day after sample preparation. The straight lines are fits indicating the linear increase of the amount of the bottom phase with the increasing concentration of spheres.

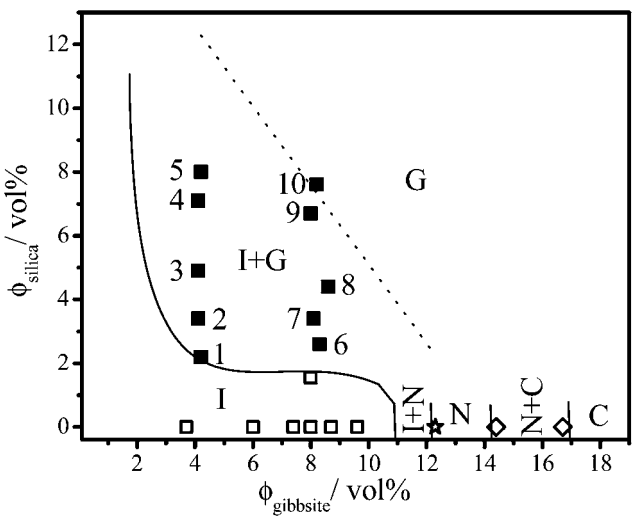

Fig. 5 Experimental phase diagram of aqueous gibbsite/silica suspensions, $D_{gibbsite}/D_{silica} = 13.8$. Open symbols represent the samples which reached equilibrium (either stayed isotropic or formed liquid-crystalline phases). Filled symbols mark the samples which did not crystallize, however, showed a phase separation with a very rigid turbid glass, G, at the bottom of their tubes. Numbers label the samples as shown in Fig. 3. Samples studied with μradXRD (discussed in detail in Section IV) are labelled 6–10 in the diagram. Phase boundaries depicted as solid lines were found experimentally. The dashed line is the glass transition line as extrapolated from Fig. 4.

is given for samples 7 and 9 as the representatives for the samples with a low and high silica concentration, respectively.

Fig. 6a shows a 2D μradXRD scattering pattern of the bottom phase of the sample 7, containing 8.1 vol% of gibbsite and 3.4 vol% of silica. The q dependent intensity profiles $I(q)$ along the horizontal (x) and vertical (y) axes were extracted from the scattering pattern by integrating a small wedge along the respective axis and are shown in Fig. 6b. We multiplied $I(q)$ with $(qR)^2$, where R is the radius of the platelets, as it was previously suggested by Kroon *et al.*[33] In such a representation the form factor $P(q)$ of randomly oriented platelets (decays as q^{-2})[33,34] should be a straight line parallel to the x-axis. Thus, the weak scattering features originating from interparticle correlations are better emphasized.

The scattering pattern in Fig. 6a possesses a slight anisotropy which is reflected and more pronounced in the $I(q)$ profiles extracted along the x (black curve) and y (gray curve) axes (Fig. 6b). A sharp peak at low q is visible for both directions. Additionally, the horizontal profile reveals three weak peaks at an intermediate q range, while the vertical profile shows only one weak peak there. The relative positions of the four peaks along the x-axis obey the relationship $1 : \sqrt{3} : \sqrt{4} : \sqrt{7}$. Thus, the peaks can be attributed to the (100), (110), (200) and (210) Bragg reflections. This indicates that the sample has a hexagonal structure, which is built up by stacks of gibbsite platelets. The hexagonal lattice spacing, a_D, was calculated by plotting q_{hkl} values (hkl the Miller indices) of the Bragg peaks *versus* $\sqrt{(h^2 + hk + k^2)}$ (see the inset of Fig. 6b). For a hexagonal structure such a plot passes through the origin and is linear with the $\frac{4\sqrt{3}\pi}{3}\frac{1}{a_D}$ slope.[35,36] The straight line in the inset of Fig. 6b confirms the good fit of the scattering data to the hexagonal structure. The values of a_D, obtained from the slope of the fits for the horizontal and vertical (not presented here) integration directions, are 248.1 nm and 241.8 nm, respectively. The small difference can be explained by fluctuations of the particle orientations within the columns.[37] The intensity profiles in Fig. 6b show a pronounced broad peak at large q values, which can be assigned as the (001) peak corresponding to the face-to-face positional correlations between the platelets in columns, a_L. The a_L lattice spacings can be calculated from the

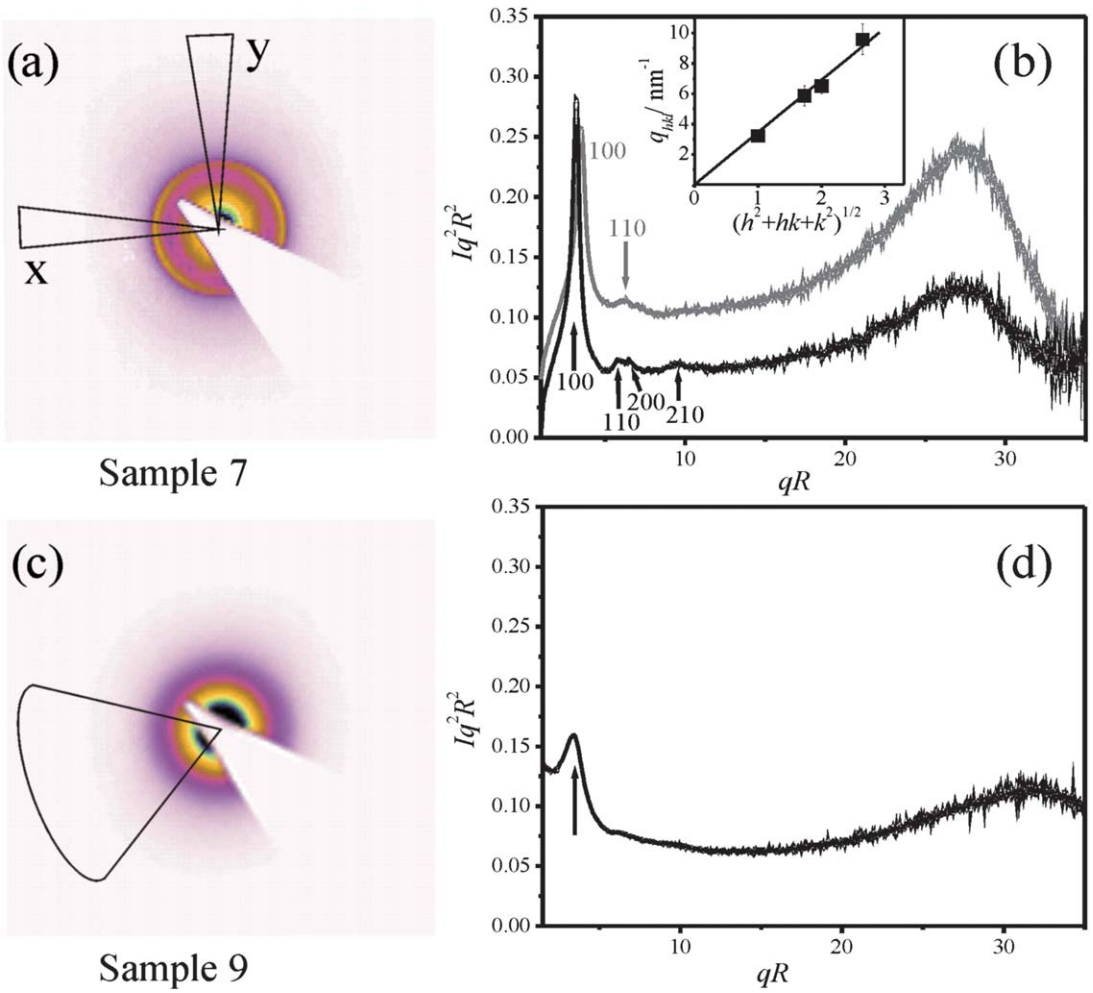

Fig. 6 The 2D μradXRD scattering pattern (a) and the intensity profiles along the x (black curve) and y (gray curve) axes (b) obtained from the glass phase of sample 7. The inset depicts the q values of the Bragg reflections *vs.* $\sqrt{(h^2 + hk + k^2)}$ for the horizontal integration direction. The straight line passing through the origin indicates a good fit of the scattering reflections to the hexagonal structure. The scattering pattern (c) and the corresponding average intensity profile (d) from the glass phase of sample 9.

$q_{(001)}$ values as $a_L = 2\pi/q_{(001)}$ and are almost identical for both the horizontal (27.4 nm) and vertical (27.1 nm) integration directions.

The presented scattering data show that the bottom phase of sample 7 has pockets of liquid-crystalline columnar stacks in hexagonal pattern. However, the whole bottom phase could not reach a full equilibrium columnar phase. The liquid-crystalline domains here are small in size and arrested in a more disordered glassy structure around them. Due to the kinetical arrest they are not able to grow further, by either taking in new platelets or annealing with their neighbours. Using the full width of the (100) peak at its half height we estimated the positional order in the bottom layer of sample 7 as extending over 1300 nm. This distance equals only five particle diameters, indicating that the positional order there is significantly shorter than in a case of the equilibrium columnar phase.[27] Here we can additionally recall the different flow properties of the equilibrium columnar phase and the present glass phase. While the former would flow when the capillary is tilted, the latter one did not, due to the high rigidity of this arrested state.

Fig. 6c presents the 2D μradXRD scattering pattern from the glass phase of sample 9 with a higher sphere concentration. Unlike the anisotropic 2D pattern from the sample 7 (Fig. 6a) this pattern is isotropic. The corresponding average scattering intensity profile is plotted in Fig. 6d and shows a drop in the intensity for the low q peak and no higher order Bragg peaks can be found there. This indicates that the bottom phase in this suspension with a higher sphere concentration is a glass with an isotropic structure. The estimated positional order in this structure is only 700 nm, two times shorter than in sample 7. The side-to-side correlation distance in this phase is determined to be 253.7 nm. The broad peak found at large q indicates the face-to-face distance to be 23.2 nm. The a_D distance in the bottom phase is slightly larger than that of sample 7. This is due to the fact that here the structure is more disordered caused by stronger attraction. At the same time a larger amount of platelets has to be accommodated than in sample 7, which results in the faces to be pushed closer together and the a_L distance becomes smaller. The positions, widths and heights of the peaks of the sample 9 glass are nearly the same for all measured vertical positions along the capillary, showing that the side-to-side and the face-to-face spacings do not change through this phase. For sample 10 the side-to-side and the face-to-face spacings of the glass were also found to remain the same along the capillary. Thus, the structure is very rigid and incompressible towards the bottom of the capillary, indicating a strongly arrested glass. Additionally, this finding complies with the rheological measurements on attractive glasses in polymer/sphere mixtures showing that these have a very high yield stress.[38]

For samples 6–8 a different result is found for the positions of the low q range peaks. Here a slight shift to lower q values is observed as the glass phase of the sample is scanned from the bottom to the top, indicating that the side-to-side correlation distances between platelets slowly increase in this direction (see Fig. 7). This means that the structure is slightly compressed to the bottom of the capillary as a result of osmotic pressure. This effect has also been observed on the sphere/platelet system forming an equilibrium liquid-crystalline phase.[27] Adding more and more spheres, and hence more attraction, to the sample

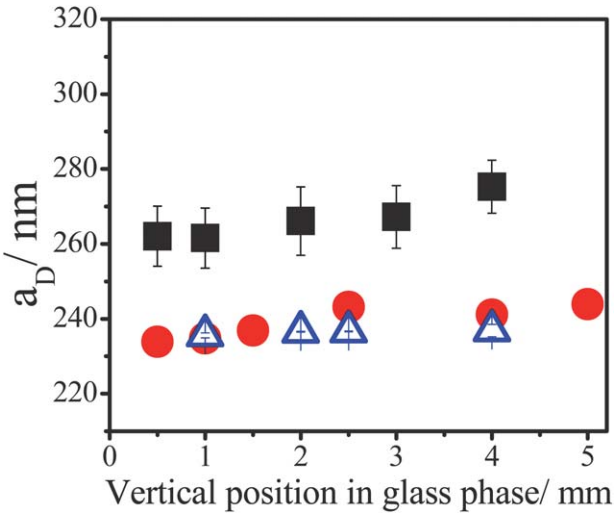

Fig. 7 The side-to-side, a_D, spacings as a function of the vertical position along the glass phase in mixed gibbsite/silica suspensions. Squares, circles and triangles are the spacings of the samples 6–8, respectively.

leads to a less and less compressible bottom phase, until, like in case of samples 9 and 10, it becomes strongly arrested and incompressible. The structure of the glass is disordered and very rigid there.

In Fig. 8a and b the side-to-side and the face-to-face spacings from the glass layer in mixed silica/gibbsite samples with a constant amount of gibbsite (8 vol%) are compared. Since in samples 6–8 the side-to-side spacing increased towards the top of the glass phase, the values from the bottom of the capillary were taken. The face-to-face correlation distances were constant along the length of the bottom phase for all samples and no specific point was selected. As can be seen in Fig. 8, increasing the concentration of spheres (up to 4.5 vol%) in the mixed gibbsite/silica samples leads to a pronounced decrease of both the side-to-side and face-to-face spacings. The lowest a_D value in sample 7 is 234.8 nm, which means that here the platelets are almost touching with their sides (D_{gibbsite} = 232.5 nm). A further increase in silica concentration leads to a slight increase in the a_D, while the a_L distance almost does not change and reaches a plateau. This can be explained by the fact that going from samples 6 to 10 (2.2–7.6 vol%) the glass phase has to accumulate more and more platelets. As a result the a_D decreases for samples 6–8, where the bottom phase consists of more ordered liquid-crystalline pockets embedded in the disordered glass. While for sample 9 and 10 where a totally disordered glass phase is present, the platelets are not filling up the space effectively. Thus, the side-to-side spacing appears larger there.

V. Discussion and conclusions

On the basis of visual observations and μradXRD measurements we presented an experimental phase and arrested state diagram of mixed suspensions of charged gibbsite platelets and silica spheres (Fig. 5). All pure gibbsite suspensions reached equilibrium and showed rich phase behaviour with the expected isotropic, nematic and columnar phases. Spherical depletants were added to the initially isotropic gibbsite suspensions to

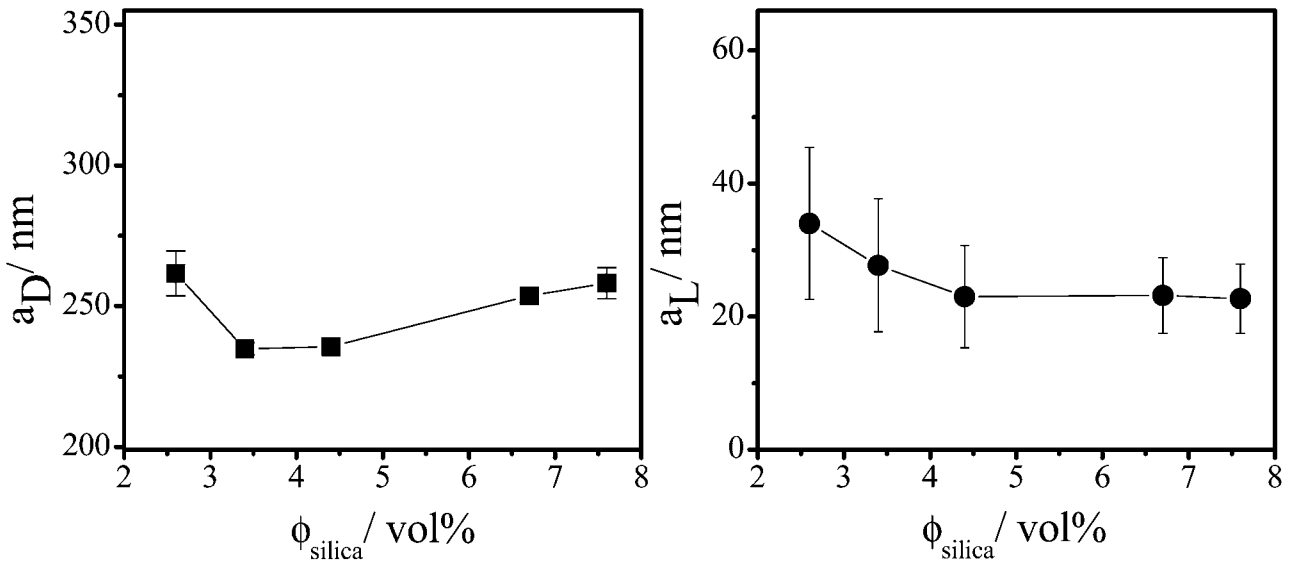

Fig. 8 The side-to-side, a_D, and the face-to-face, a_L, correlation distances as a function of the silica volume percent in mixed gibbsite/silica samples with a constant amount of gibbsite (8 vol%). Samples were labelled 6–10 in the experimental phase diagram in Fig. 5.

manipulate their phase behaviour. Unlike a previous study, where depletion attraction in gibbsite suspensions expands the isotropic/columnar phase coexistence region,[27] here the system hits the glass transition line before being able to form the equilibrium liquid-crystalline phase. A glass phase formed in the mixed samples at the bottom of the capillaries and coexisted with an isotropic phase above. Simple test tube inversion experiments showed the strong rigidity and the arrested nature of this state. The time needed for the glass formation decreased with increasing the amount of spheres in the samples. As the driving force of this glass formation is the induced depletion attraction it proceeded slower in mixtures with a lower depletant concentration. During the glass phase formation in samples with low depletant concentrations the gibbsite platelets had enough time and space around them to partially form a liquid-crystalline phase, due to the relatively weak attraction. However, these small regions became frozen in the disordered glassy structure around them. Due to the kinetical arrest the formed liquid-crystalline pockets were not able to anneal, take new platelets in and reorganize themselves in an equilibrium ordered structure. The size of such liquid-crystalline pockets decreased with an increasing attraction in the system. Until at high depletant concentrations they became so small or did not appear at all, that the glass phase can be regarded as totally disordered and having an isotropic structure. Similarly, in polymer/spherical colloid mixtures it was found that crystallites become smaller as the depletion attraction strengthens and disappear at the arrested state threshold.[39]

In Fig. 9 the evolution of the structure of the arrested state in platelet/sphere mixtures is summarized on the basis of their scattering intensity profiles. There are several gradual changes in the $I(q)$ upon increasing the sphere concentration in samples. The clearest change is in the height of the first scattering peak, as it decreases with higher sphere concentration. This trend has been observed in sphere/polymer mixtures[15] before and is theoretically predicted for attractive glass systems,[40] since they form due to the clustering of the particles. Such clustering would lead to the decrease of the average number of the neighbours, which further would lead to more inhomogeneous structure.[15] This is reflected in the decrease of the first scattering peak. Furthermore, the Bragg peaks of high order in the $I(q)$ become weaker and broader, until in samples with the highest concentration of spheres (samples 9 and 10) they do not appear in the intensity profile anymore. These changes suggest that the liquid-crystalline pockets of hexagonal structure present in the glass phase decrease in size with increasing attraction, until they disappear in samples with the highest attraction and indicate that for these the glass phase has an isotropic structure. Additionally, the scattering intensity profiles for the samples with the strongest depletion attraction (9 and 10), show an upturn at low q. The low q upturn indicates the presence of density fluctuations on the scale larger than the particle size. These fluctuations are indeed expected in the attractive glasses, as observed experimentally[15,38] and predicted by theory.[41,42]

We will discuss in detail the role of the strength and the range of the depletion attraction on the glass formation in platelet suspensions. First, we estimate the strength of the depletion attraction between two hexagonal platelets of an area $A_{platelet}$:

$$A_{platelet} = \frac{3\sqrt{3}}{8} D_{platelet}^2 \quad (1)$$

with $D_{platelet}$ being the diameter of a platelet. When the platelets are immersed in a suspension of spheres with a volume fraction ϕ_{sphere} a depletion attraction will occur between the platelets. It will be at a maximum when the platelets contact each other face-to-face[43] and is given by the following equation:

$$\frac{W_{depl}(\text{contact})}{k_B T} = -\frac{\phi_{sphere}}{V_{sphere}} D_{sphere} A_{platelet} \quad (2)$$

where $k_B T$ is the thermal energy and $V_{sphere} = \frac{\pi}{6} D_{sphere}^3$ is the sphere volume. Combining eqn (1) and (2) we can write:

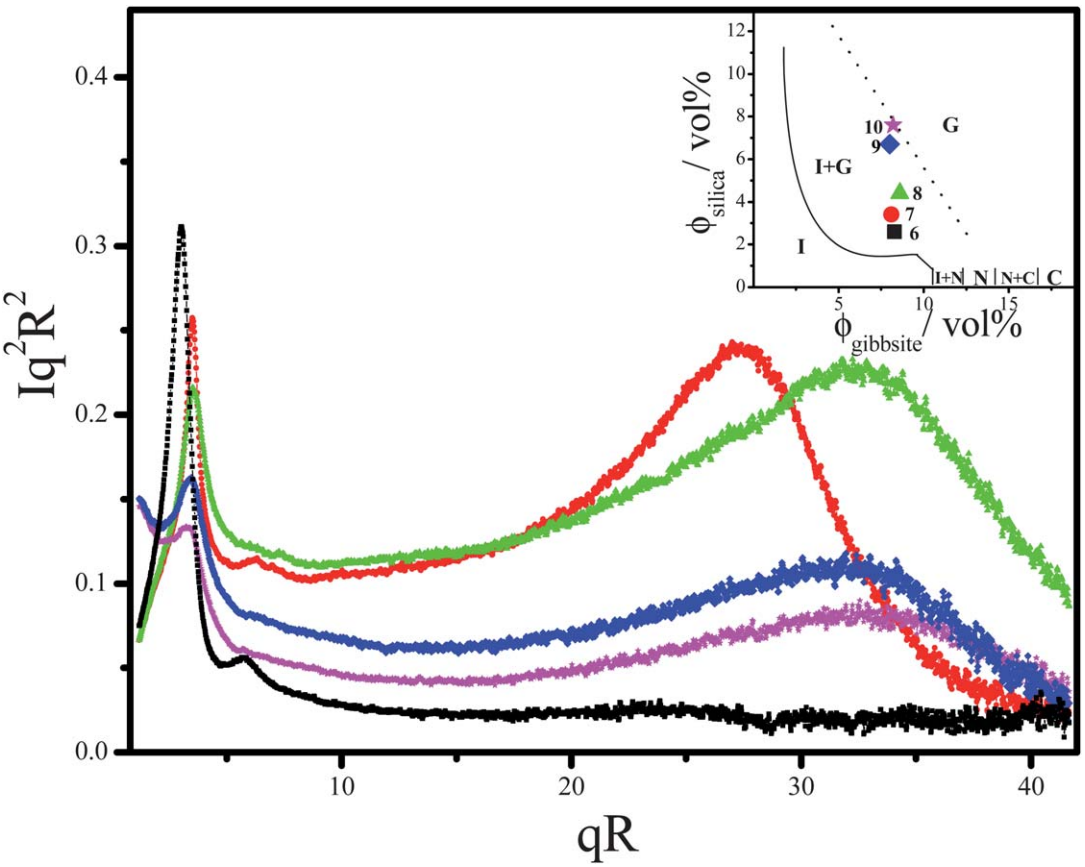

Fig. 9 The scattering intensity profiles along the horizontal direction of the glass phase of samples: 6 (black squares), 7 (red circles), 8 (green triangles), 9 (blue diamonds), and 10 (magenta stars). The inset represents general features of the phase diagram (shown in detail in Fig. 5) and the positions of the studied samples in it.

$$\frac{W_{\mathrm{depl}}(\mathrm{contact})}{k_{\mathrm{B}}T} = -\frac{9\sqrt{3}}{4\pi}\phi_{\mathrm{sphere}}\left(\frac{D_{\mathrm{platelet}}}{D_{\mathrm{sphere}}}\right)^{2} \qquad (3)$$

Eqn (3) shows that the ratio of the platelet to the sphere diameter (in this study $D_{\mathrm{gibbsite}}/D_{\mathrm{silica}} = 13.8$) strongly affects the depth of the depletion potential. In this system silica Ludox CL spheres at concentrations between 2.2 and 8.0 vol% would induce a strong depletion attraction between the platelets with contact values ranging between 5.2 and 19.0 $k_{\mathrm{B}}T$. These attraction values can be compared to the results from the previous study, where smaller gibbsite platelets were mixed with the same spheres.[27] Here the ratio $D_{\mathrm{gibbsite}}/D_{\mathrm{silica}}$ is 13.8 compared to 5.7 then, which is almost two and a half times larger. This explains why, despite the same volume percent of spheres, the depletion attraction was significantly weaker there (its largest contact value was 3.2 $k_{\mathrm{B}}T$). Therefore, it is not surprising that the glass state was not found in the previous system, as according to theory the attractive glass formation happens at a strong enough attraction strength.[9]

However, not only the strength of the attraction affects the arrested state formation but also the range compared to the range of the hard core repulsion between the particles is of importance as well. Theoretical calculation, existing only for spherical colloids, shows that glass formation will take place in systems with a short range attraction of approximately 10% of the hard core repulsion.[12,44] The range of the depletion attraction is related to the size of the depletant,[21] which in this case is the diameter of the silica spheres. Thus, for the gibbsite platelets ($D_{\mathrm{gibbsite}} = 232.5$ nm) and Ludox CL spheres ($D_{\mathrm{silica}} = 16.8$ nm) used in this study the range of attraction is approximately 7% of the hard core repulsion. While, for the previous study with smaller gibbsite platelets ($D_{\mathrm{gibbsite}} = 95.0$ nm) this was approximately 17%. This can be another reason why the attractive glass was not found in these suspensions.

To summarize, detailed information was obtained from the μradXRD measurements about the structure of the arrested state formed due to a strong short-ranged depletion attraction in aqueous mixtures of gibbsite platelets and silica spheres. It is shown that the arrested state is an attractive glass. To our knowledge, this is the first experimental study in which the formation of the attractive glass in suspensions of colloidal platelets was observed. Thus, our experimental platelet system opens new possibilities to model the arrested state behaviour of platelet-like clay particles. Their suspensions are known to form arrested states at very low concentrations,[7] while the liquid-crystalline phases could be found only seldom.[45] The use of depletion offers us an effective control over the strength and the range of the attraction in the system providing a possibility to tune between the liquid-crystalline and the arrested state formation in platelet suspensions. An additional option to tune the glass formation would be the manipulation of the repulsion between the platelets by changing the salt concentration in suspensions.

Acknowledgements

We thank Mark Vis for his help with the AFM measurements. Peter Holmqvist is thanked for many fruitful discussions and a careful reading of the manuscript. The team of BM-26, Dima Byelov, and Anatoly Snigirev are thanked for their technical assistance during the synchrotron experiments. This work is part of the research program of the Foundation for Fundamental Research on Matter (FOM), which is part of the Netherlands Organization for Scientific Research (NWO). NWO is acknowledged for granting the beam time.

References

1 E. Dickinson, *An Introduction to Food Colloids*, Oxford University Press, Oxford, England, 1992.
2 H. H. Murray, *Appl. Clay Sci.*, 2000, **17**, 207–221.
3 G. C. Maitland, *Curr. Opin. Colloid Interface Sci.*, 2000, **5**, 301–311.
4 H. C. H. Darley and G. R. Gray, *Composition and Properties of Drilling and Completion Fluids*, Gulf Professional Publishing, Huston, TX, 1988.
5 P. Davidson and J.-C. P. Gabriel, *Curr. Opin. Colloid Interface Sci.*, 2005, **9**, 377–383.
6 M. J. Solomon and P. T. Spicer, *Soft Matter*, 2010, **6**, 1391–1400.
7 H. Tanaka, J. Meunier and D. Bonn, *Phys. Rev. E: Stat., Nonlinear, Soft Matter Phys.*, 2004, **69**, 031404.
8 E. Zaccarelli, *J. Phys.: Condens. Matter*, 2007, **19**, 323101.
9 F. Sciortino and P. Tartaglia, *Adv. Phys.*, 2005, **54**, 471.
10 K. A. Dawson, *Curr. Opin. Colloid Interface Sci.*, 2002, **7**, 218–227.
11 P. N. Pusey and W. van Megen, *Phys. Rev. Lett.*, 1987, **59**, 2083–2086.
12 F. Sciortino, *Nat. Mater.*, 2002, **1**, 145–146.
13 P. N. Pusey and W. van Megen, *Nature*, 1986, **320**, 340–342.
14 P. N. Pusey, in *Liquids, Freezing and Glass Transition*, ed. J.-P. Hansen and D. Levesque, North-Holland, Amsterdam, 1991, pp. 765–942.
15 K. N. Pham, S. U. Egelhaaf, P. N. Pusey and W. C. K. Poon, *Phys. Rev. E: Stat., Nonlinear, Soft Matter Phys.*, 2004, **69**, 011503.
16 K. N. Pham, A. M. Puertas, J. Bergenholtz, S. U. Egelhaaf, A. Moussaid, P. N. Pusey, A. B. Schofield, M. E. Cates, M. Fuchs and W. C. K. Poon, *Science*, 2002, **296**, 104–106.
17 T. Eckert and E. Bartsch, *Phys. Rev. Lett.*, 2002, **89**, 125701.
18 X. H. Lu, S. G. J. Mochrie, S. Narayanan, A. R. Sandy and M. Sprung, *Phys. Rev. Lett.*, 2008, **100**, 045701.
19 S. H. Chen, W. R. Chen and F. Mallamace, *Science*, 2003, **300**, 619–622.
20 E. Zaccarelli, C. Mayer, A. Asteriadi, C. N. Likos, F. Sciortino, J. Roovers, H. Iatrou, N. Hadjichristidis, P. Tartaglia, H. Lowen and D. Vlassopoulos, *Phys. Rev. Lett.*, 2005, **95**, 268301.
21 S. Asakura and F. Oosawa, *J. Polym. Sci.*, 1958, **33**, 183–192.
22 A. M. Wierenga, T. A. J. Lenstra and A. P. Philipse, *Colloids Surf., A*, 1998, **134**, 359–371.
23 A. V. Petukhov, D. van der Beek, R. P. A. Dullens, I. P. Dolbnya, G. J. Vroege and H. N. W. Lekkerkerker, *Phys. Rev. Lett.*, 2005, **95**, 077801.
24 F. M. van der Kooij, K. Kassapidou and H. N. W. Lekkerkerker, *Nature*, 2000, **406**, 868–871.
25 D. van der Beek and H. N. W. Lekkerkerker, *Langmuir*, 2004, **20**, 8582–8586.
26 H. van Olpen, *An Introduction to Clay Colloid Chemistry*, Interscience, New York, 1963.
27 D. Kleshchanok, A. V. Petukhov, P. Holmqvist, D. V. Byelov and H. N. W. Lekkerkerker, *Langmuir*, 2010, **26**, 13614–13621.
28 J. E. G. Wijnhoven, *J. Colloid Interface Sci.*, 2005, **292**, 403–409.
29 M. Borsboom, W. Bras, I. Cerjak, D. Detollenaere, D. G. van Loon, P. Goedtkindt, M. Konijnenburg, P. Lassing, Y. K. Levine, B. Munneke, M. Oversluizen, R. van Tol and E. Vlieg, *J. Synchrotron Radiat.*, 1998, **5**, 518–520.
30 A. V. Petukhov, J. H. J. Thijssen, D. C. 't Hart, A. Imhof, A. van Blaaderen, I. P. Dolbnya, A. Snigirev, A. Moussaid and I. Snigireva, *J. Appl. Crystallogr.*, 2006, **39**, 137–144.
31 A. Snigirev, V. Kohn, I. Snigireva and B. Lengeler, *Nature*, 1996, **384**, 49–51.
32 J. A. C. Veerman and D. Frenkel, *Phys. Rev. A: At., Mol., Opt. Phys.*, 1992, **45**, 5632–5648.
33 M. Kroon, W. L. Vos and G. H. Wegdam, *Phys. Rev. E: Stat. Phys., Plasmas, Fluids, Relat. Interdiscip. Top.*, 1998, **57**, 1962–1970.
34 B. J. Lemaire, P. Panine, J. C. P. Gabriel and P. Davidson, *Europhys. Lett.*, 2002, **59**, 55–61.
35 T. Hahn, *International Tables for Crystallography*, Reidel, Dortrecht, 1983.
36 P. Holmqvist, P. Alexandridis and B. Lindman, *Langmuir*, 1997, **13**, 2471–2479.
37 M. C. D. Mourad, A. V. Petukhov, G. J. Vroege and H. N. W. Lekkerkerker, *Langmuir*, 2010, **26**, 14182–14187.
38 K. N. Pham, G. Petekidis, D. Vlassopoulos, S. U. Egelhaaf, W. C. K. Poon and P. N. Pusey, *J. Rheol. (Melville, NY, U. S.)*, 2008, **52**, 649–676.
39 S. M. Ilett, A. Orrock, W. C. K. Poon and P. N. Pusey, *Phys. Rev. E: Stat. Phys., Plasmas, Fluids, Relat. Interdiscip. Top.*, 1995, **51**, 1344–1352.
40 K. A. Dawson, G. Foffi, M. Fuchs, W. Goetze, F. Sciortino, M. Sperl, P. Tartaglia, T. Voigtmann and E. Zaccarelli, *Phys. Rev. E: Stat. Phys., Plasmas, Fluids, Relat. Interdiscip. Top.*, 2000, **63**, 011401.
41 M. E. Cates, M. Fuchs, K. Kroy, W. C. K. Poon and A. M. Puertas, *J. Phys.: Condens. Matter*, 2004, **16**, S4861–S4875.
42 G. Fritz-Popovski, *J. Chem. Phys.*, 2009, **131**, 114902.
43 T. G. Mason, *Phys. Rev. E: Stat., Nonlinear, Soft Matter Phys.*, 2002, **66**, 060402.
44 J. Bergenholtz, W. C. K. Poon and M. Fuchs, *Langmuir*, 2003, **19**, 4493–4503.
45 L. J. Michot, I. Bihannic, S. Maddi, S. S. Funari, C. Baravian, P. Levitz and P. Davidson, *Proc. Natl. Acad. Sci. U. S. A.*, 2006, **103**, 16101–16104.

